IOP Conference Series: Materials Science and Engineering

PAPER • OPEN ACCESS

The influence of slip effects on peristaltic transport of a Rabinowitsch fluid model in a non uniform tube

To cite this article: K Thanesh Kumar and A Kavitha 2017 *IOP Conf. Ser.: Mater. Sci. Eng.* **263** 062004

IOP Conf. Series: Materials Science and Engineering **263** (2017) 062004 doi:10.1088/1757-899X/263/6/062004

The influence of slip effects on peristaltic transport of a Rabinowitsch fluid model in a non uniform tube

K Thanesh Kumar and A Kavitha
Department of Mathematics, School of Advanced Sciences, VIT University, Vellore-632014.

E-mail: kavitha@vit.ac.in

Abstract: The present article deals with the Peristaltic flow of a Rabinowitsch fluid model is considered in a non uniform tube with slip effects. Wall properties analysis is also taken into account. Here the governing equations for Rabinowitsch fluid model are simplified by using long wavelength approximation and low Reynolds number and dynamic boundary conditions, analytical expressions have been obtained stream function, temperature profile, and velocity distribution. The effects of various physical parameters on stream function, temperature profile and velocity are analyzed through graphs and the results are discussed in detail.

1. Introduction

A variety of complex rheological fluids can easily be transported from one place to another place with a special type of pumping known as Peristaltic Pumping. This pumping principle is called Peristalsis. The mechanism includes involuntary periodic contraction followed by relaxation or expansion of the ducts the fluids move through. This leads to the rise in pressure gradient that eventually pushed the fluid forward. This type of pumping is first observed in physiology where food moves through the digestive tract, urine transport from the kidney to the bladder through ureters, semen moves through the vas deferens, lymphatic fluids moves through lymphatic vessels, bile flows from the gall bladder into the duodenum, spermatozoa move through the ducts efferentes of the male reproductive tract and cervical canal, ovum moves through the fallopian tube, and blood circulates in small blood vessels. Historically, however, the engineering analysis of peristalsis was initiated much later than in physiological studies. Applications in industrial fluid mechanics are like aggressive chemicals, high solid slurries, noxious fluid and other materials that are transported by peristaltic pumps. Roller pumps, hose pumps, tube pumps, ginger pumps, heart lung machines, blood pump machines, and dialysis machines are engineered on the basis of peristalsis.

The study of peristalsis has received considerable attention in the last few decades mainly because of its relevance of engineering and biological systems. Several studies have been made analyzing both theoretical and experimental aspects of the peristaltic motion of Newtonian and non Newtonian fluids in different situations Fung and Yih [1], Shapiro et al. [2], Radhakrishnamacharya [3], Misery et al. [4], Mishra et al. [5], Srinivasaacharya et al. [6], Hayat et al. [7], Kothandapani et al. [8], sobh [9]. Sinha et.al [10] debated peristaltic flow of MHD and heat transfer in an asymmetric channel in the presence of variable viscosity, velocity-slip and temperature jump conditions. Kavitha et al. [11] studied the peristaltic transport of a Jeffrey fluid between porous walls with suction and injection. Eladabe et.al [12] analyzed the MHD peristaltic flow of a couple stress fluids with heat and mass transfer in a porous medium. Dheia et.al [13] discussed the peristaltic flow of a Jeffrey fluid in a porous medium channel with wall properties and heat transfer. Kavitha et al. [14] discussed the peristaltic transport of Jeffrey fluid in contact with Newtonian fluid in an inclined channel. Saravana et al. [15] discussed influence of slip, wall properties and heat transfer on MHD peristaltic transport of Jeffrey fluid in a non uniform porous channel. Saravana et al. [16] discussed influence of slip, heat and mass transfer on peristaltic transport of third order fluid in an inclined asymmetric channel. Hemadri Reddy et al. [17] studied the velocity slip effects on MHD peristaltic pumping of a Prandtl fluid in a non uniform channel.

We deliberate here on the Rabinowitsch fluid model. Rabinowitsch fluid model is one of the fluid models where there exists a non linear relationship between the shear stress and strain rate. This fluid model has its significance as the three major categories for fluid are depicted for different values of non linear factor γ, for $\gamma = 0$ this model represents Newtonian fluids, for $\gamma < 0$ it represents shear thickening fluids, and for $\gamma > 0$ it exhibits the behavior of shear thinning fluids. The experimental validation for this model was offered by Wada et al. [18]. Singh et.al [19] adopted Rabinowitsch fluid model to discuss the performance of pivoted curved slider bearings. Akbar et al. [20] discussed the applications of Rabinowitsch fluid model for peristalsis. Further investigations in the peristaltic motion of Rabinowitsch fluid model can be gathered in Refs [21-25].

The application of Rabinowitsch fluid model in peristalsis is very useful in physiology and biomedicine as it is involved in pumping of blood in heart/lung machines. Recently, heat transfer in peristalsis has gained much importance due to its numerous applications in engineering and biomedical sciences. Heat transfer comprises many complicated processes such as assessing skin burns, destruction of undesirable cancer tissues, dilution technique in examining blood flow, paper making, vasodilatation, food processing, metabolic heat generation and radiation between surface and its environment. It may be noticed that blood flow increases when a man does hard physical exercises also when the body is exposed to excessive heat environment. In order to take care of the increase in blood flow, the dimensions of the artery have to increase suitably. Sinha et al. [26] discussed peristaltic flow of MHD and heat transfer in an asymmetric channel in the presence of variable viscosity, velocity slip and temperature jump conditions. Eldabe et al. [27] analyzed the MHD peristaltic flow of a couple stress fluids with heat and mass transfer in a porous medium.

2. Mathematical Formulation

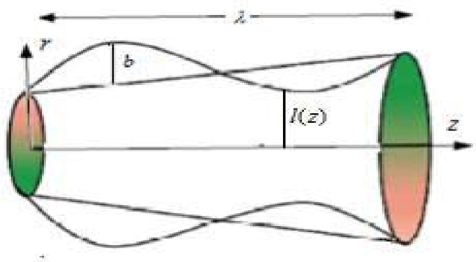

Figure 1. Physical model

IOP Conf. Series: Materials Science and Engineering **263** (2017) 062004 doi:10.1088/1757-899X/263/6/062004

Here we have considered the peristaltic motion phenomenon for the two dimensional flow of an incompressible fluid in a non-uniform tube. The equations for conservation of mass, momentum and energy be written as

$$\frac{\partial \tilde{u}}{\partial \tilde{r}}+\frac{\tilde{u}}{\tilde{r}}+\frac{\partial \tilde{w}}{\partial \tilde{z}}=0 \tag{1}$$

$$\rho\left(\frac{\partial \tilde{u}}{\partial \tilde{t}}+\tilde{u}\frac{\partial \tilde{u}}{\partial \tilde{r}}+\tilde{w}\frac{\partial \tilde{u}}{\partial \tilde{z}}\right)=-\frac{\partial \tilde{p}}{\partial \tilde{r}}+\frac{1}{\tilde{r}}\frac{\partial(\tilde{r}\tau_{\tilde{r}\tilde{r}})}{\partial \tilde{r}}+\frac{\partial(\tau_{\tilde{r}\tilde{z}})}{\partial \tilde{z}}-\frac{\tau_{\tilde{z}\tilde{z}}}{\tilde{r}} \tag{2}$$

$$\rho\left(\frac{\partial \tilde{w}}{\partial \tilde{t}}+\tilde{u}\frac{\partial \tilde{w}}{\partial \tilde{r}}+\tilde{w}\frac{\partial \tilde{w}}{\partial \tilde{z}}\right)=-\frac{\partial \tilde{p}}{\partial \tilde{z}}+\frac{1}{\tilde{r}}\frac{\partial(\tilde{r}\tau_{\tilde{r}\tilde{z}})}{\partial \tilde{r}}+\frac{\partial(\tau_{\tilde{z}\tilde{z}})}{\partial \tilde{z}} \tag{3}$$

$$\rho C_p\left(\frac{\partial \tilde{T}}{\partial \tilde{t}}+\tilde{u}\frac{\partial \tilde{T}}{\partial \tilde{r}}+\tilde{w}\frac{\partial \tilde{T}}{\partial \tilde{z}}\right)=k_1\left(\frac{\partial^2 \tilde{T}}{\partial \tilde{r}^2}+\frac{1}{\tilde{r}}\frac{\partial \tilde{T}}{\partial \tilde{r}}+\frac{\partial^2 \tilde{T}}{\partial \tilde{z}^2}\right)+\tau_{\tilde{r}\tilde{r}}\left(\frac{\partial \tilde{u}}{\partial \tilde{r}}\right)+\tau_{\tilde{z}\tilde{z}}\left(\frac{\partial \tilde{u}}{\partial \tilde{z}}\right)+\tau_{\tilde{r}\tilde{z}}\left(\frac{\partial \tilde{w}}{\partial \tilde{r}}+\frac{\partial \tilde{u}}{\partial \tilde{z}}\right) \tag{4}$$

Where ρ is the density, $\tilde{u}$ and $\tilde{w}$ are the respective velocity components in radial and axial directions respectively, C_p is specific heat.

The corresponding boundary conditions for the problem as shown in Figure (1) are defined as

$$\tilde{w}=-c+\beta_1\frac{\partial \tilde{w}}{\partial \tilde{r}}, at\ \tilde{r}=\tilde{H}=l(\tilde{z})+b\sin\frac{2\pi}{\lambda}(\tilde{z}-c\tilde{t}),$$
$$\frac{\partial \tilde{w}}{\partial \tilde{r}}=0, at\ \tilde{r}=0 \tag{5}$$

Where $\tilde{H}$ is the non-uniform wave in which $l(\tilde{z})$ is the non-uniform radius, b is the wave amplitude.

$$-k_1\frac{\partial \tilde{T}}{\partial \tilde{r}}=\eta_d\left(\tilde{T}-\tilde{T}_0\right) at\ \tilde{r}=\tilde{H}, \frac{\partial \tilde{T}}{\partial \tilde{r}}=0, at\ \tilde{r}=0 \tag{6}$$

The non-dimensional quantities are

$$r=\frac{\tilde{r}}{l_2}, z=\frac{\tilde{z}}{\lambda}, w=\frac{\tilde{w}}{c}, u=\frac{\lambda\tilde{u}}{l_2 c}, \tau_{rz}=\frac{l_2\tau_{\tilde{r}\tilde{z}}}{c\mu}, \tau_{rr}=\frac{l_2\tau_{\tilde{r}\tilde{r}}}{c\mu},$$

$$\varepsilon=\frac{b}{l_2}, \tau_{zz}=\frac{l_2\tau_{\tilde{z}\tilde{z}}}{c\mu}, \delta=\frac{l_2}{\lambda}, p=\frac{l_2{}^2 p}{c\lambda\mu}, t=\frac{c\tilde{t}}{\lambda}, R_e=\frac{l_2 c\rho_f}{\mu_f}, \tag{7}$$

$$\theta=\frac{\tilde{T}-\tilde{T}_0}{\tilde{T}_0}, l(\tilde{z})=l_2+k\tilde{z}, h=\frac{\tilde{H}}{l_2}=1+\frac{\lambda kz}{l_2}+\varepsilon\sin(2\pi(z-t)),$$

$$E_1=\frac{-\sigma l_2{}^3}{\lambda^3\mu c}, E_2=\frac{m l_2{}^3 c}{\lambda^3 c}, E_3=\frac{C l_2{}^3}{\lambda^2\mu}, B_r=\frac{\eta_d c^2}{\tilde{T}_0 l_2{}^2}, k=\frac{\eta_d l_2}{k_1}, \beta_1=\frac{\tilde{\beta}_1}{l_2}.$$

Under the assumption of low Reynolds number and long wave length approximation, dropping bars and terms containing R_e, δ using (7) into the equations (1-6) we get the following equations

$$\frac{\partial u}{\partial r}+\frac{u}{r}+\frac{\partial w}{\partial z}=0 \tag{8}$$

$$R_e\delta^3\left(u\frac{\partial u}{\partial r}+w\frac{\partial u}{\partial z}\right)=-\frac{\partial p}{\partial r}+\delta^2\frac{\partial(\tau_{rz})}{\partial z}+\frac{\delta}{r}\frac{\partial(r\tau_{rr})}{\partial r}-\frac{\delta}{r}\tau_{\theta\theta} \tag{9}$$

$$R_e\delta\left(u\frac{\partial w}{\partial r}+w\frac{\partial w}{\partial z}\right)=-\frac{\partial p}{\partial z}+\frac{1}{r}\frac{\partial(r\tau_{rz})}{\partial r}+\delta\frac{\partial(\tau_{zz})}{\partial z} \tag{10}$$

$$R_e\delta\Pr\left(u\frac{\partial\theta}{\partial r}+w\frac{\partial\theta}{\partial z}\right)=\left[\frac{1}{r}\frac{\partial\theta}{\partial r}+\frac{\partial^2\theta}{\partial r^2}+\delta^2\left(\frac{\partial^2\theta}{\partial z^2}\right)\right]+Br\left(\delta\tau_{rr}\frac{\partial u}{\partial r}+\delta^2\tau_{rz}\frac{\partial u}{\partial z}+\tau_{rz}\left(\frac{\partial w}{\partial r}+\delta^2\frac{\partial u}{\partial z}\right)\right) \tag{11}$$

$$w=-1+\beta_1\frac{\partial w}{\partial r},\quad \text{at } r=h(z)=1+\frac{\lambda kz}{l_2}+\varepsilon\sin 2\pi(z-t)$$

$$\frac{\partial w}{\partial r}=0\ ,\ \text{at } r=0 \tag{12}$$

$$\frac{\partial\theta}{\partial r}+k\theta=0\ \ at\, r=h,\ \frac{\partial\theta}{\partial r}=0, at\, r=0$$

The simplified equations after using long wavelength and low Reynolds number assumptions equations (9) to (12) are written as

$$\frac{\partial p}{\partial r}=0 \tag{13}$$

$$\frac{\partial p}{\partial z}=\frac{1}{r}\frac{\partial}{\partial r}\left[r\tau_{rz}\right] \tag{14}$$

$$\left(\frac{1}{r}\frac{\partial\theta}{\partial r}+\frac{\partial^2\theta}{\partial r^2}\right)+Br\,\tau_{rz}\left(\frac{\partial w}{\partial r}\right)=0 \tag{15}$$

The governing equation of motion of the flexible wall is given by

$$L(\tilde{H})=\tilde{p}-\tilde{p}_0 \tag{16}$$

Where L is the operator that is used to characterize the motion of the stretched membrane with damping forces and p_0 is the pressure on the outside surface of the wall due to tension in the muscle, which is assumed to be zero, and L can be written as

$$L=-\sigma\frac{\partial^2}{\partial\tilde{z}^2}+m\frac{\partial^2}{\partial\tilde{t}^2}+C'\frac{\partial}{\partial\tilde{t}} \tag{17}$$

After dimensionless it becomes

$$\frac{\partial p}{\partial z}=\frac{\partial L(h)}{\partial z}=\left(E_1\frac{\partial^3 h}{\partial z^3}+E_2\frac{\partial^3 h}{\partial z\partial t^2}+E_3\frac{\partial^2 h}{\partial z\partial t}\right)=A(z,t) \tag{18}$$

Where τ_{rz} component is obtained by using equation (14) in the stress tensor given by

$$\frac{\partial w}{\partial r} = \tau_{rz} + \gamma(\tau_{rz})^3 \tag{19}$$

$$\frac{\partial p}{\partial z} = A(z,t),\ \tau_{rz} = 0, at\, r = 0 \tag{20}$$

2.1 Solution of the Problem

Solving equation (14) by using (20) we get

$$\tau_{rz} = \frac{rA}{2} \tag{21}$$

By substituting (21) in (19) , using (12) we get

$$w = \frac{A}{4}(r^2 - h^2) + \gamma\frac{A^3}{32}(r^4 - h^4) + \beta_1\left(\frac{hA}{2} + \gamma\frac{h^3A^3}{8}\right) - 1 \tag{22}$$

Now by solving equation (15) by using (12) we get

$$\theta = \frac{1}{96}\left(\frac{3B_rh^3A^2}{k} + \frac{B_r\gamma h^5A^4}{2k} - \frac{3B_rr^4A^2}{4} - \frac{B_r\gamma A^4r^6}{12} + \frac{3B_rh^4A^2}{4} + \frac{B_r\gamma h^4A^6}{12}\right) \tag{23}$$

Velocities in terms of stream function relation can be defined as

$$u = -\frac{1}{r}\frac{\partial\psi}{\partial z},\ w = \frac{1}{r}\frac{\partial\psi}{\partial r}\ at\ r = h \tag{24}$$

Where $A(z,t) = 8\pi^3\varepsilon\left[\left[-\cos 2\pi(z-t).(E_1+E_2)\right] + E_3\frac{\sin 2\pi(z-t)}{2\pi}\right]$ (25)

3. Results and Discussions

In this section, the effects if various emerging parameters on velocity, temperature profile and on stream functions are discussed through graphically.

The velocity profiles are plotted from Figure. (2) to (6) to study the effects of different parameters such as rigidity parameter E_1 and stiffness parameter E_2, viscous damping force parameter E_3 slip parameter β_1 and non uniform parameter k. In Fig (2), (3) are plotted for different values of rigidity parameter E_1, stiffness parameter E_2 for shear thinning and viscous cases. It is observed that velocity profiles are increases, but, opposite behavior depicted for shear thickening case. It is due to the fact that less resistance is accessible to the flow because of the wall properties and thus velocity increases, but, opposite behavior is depicted for shear thinning case gets the larger curve, and the curves for viscous fluids get smaller variations Figure. (4) is plotted for different values of viscous damping force parameter E_3. It is observed that velocity curve gets smaller variations for increasing values of E_3 and decreases for increasing values of shear thickening case, but, opposite behavior for shear thinning and viscous fluids. Figure. (5) is plotted for different values of slip parameter β_1. It is observed that velocity increases for increasing values of and slip parameter β_1. Figure. (6) is plotted for different values of non uniform parameter k. It is observed that velocity increases with increasing the values of k.

In Figure. (7) to (12) the nature of the temperature profile is presented. In Figure. (7) It is observed that the temperature profile is increasing with increasing values of Brickman number B_r, it is seen here that temperature profile is an increasing function for shear thinning, thickening and viscous fluid. Because higher values B_r there is a stronger heat generation due to friction is used by shear in the flow which raises the fluid temperature. In Figure. (8) it is observed that the temperature profile is increasing with increasing the non uniform parameter k for all the three cases . In Figure. (9) to (12) it is observed that the temperature profile is increases with increasing values of rigidity, stiffness, viscous damping force parameter, slip parameter for all increasing values of rigidity, stiffness and viscous fluid. Also we observed that variations get closed for damping force parameters for shear thickening case.

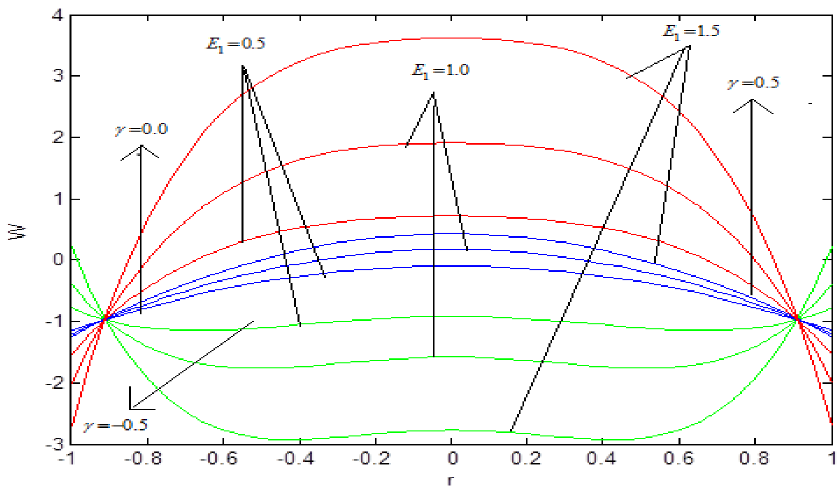

Figure 2. For fixed $E_2 = 1.0, E_3 = 0.5, \lambda = 0.02, z = 0.22, \varepsilon = 0.01, t = 0.25, l_2 = 0.34, k = 2.4$ varying $E_1 = 0.5, 1.0, 1.5,\ \gamma = -0.5, 0, 0.5$

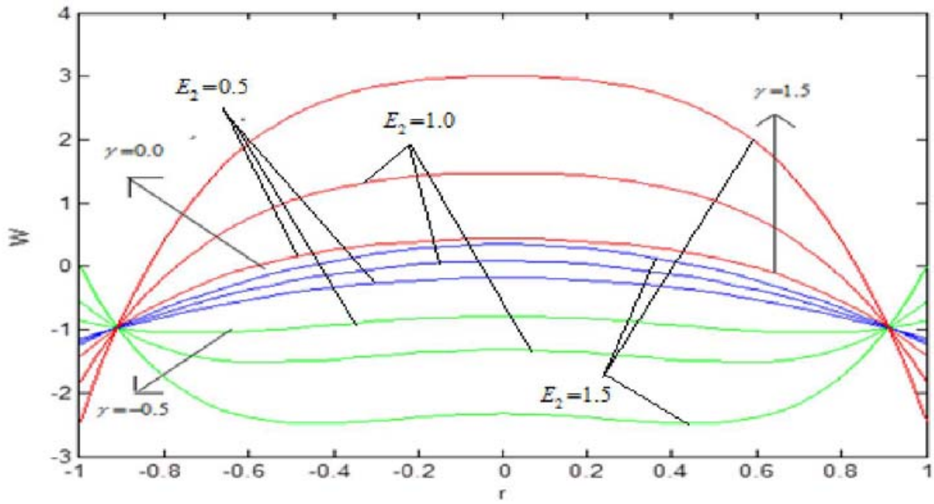

Figure 3. For fixed $E_1 = 1.0, E_3 = 0.5, \lambda = 0.02, z = 0.22, \varepsilon = 0.01, t = 0.25, l_2 = 0.34, k = 2.4$ varying $E_2 = 0.5, 1.0, 1.5,\ \gamma = -0.5, 0, 0.5$

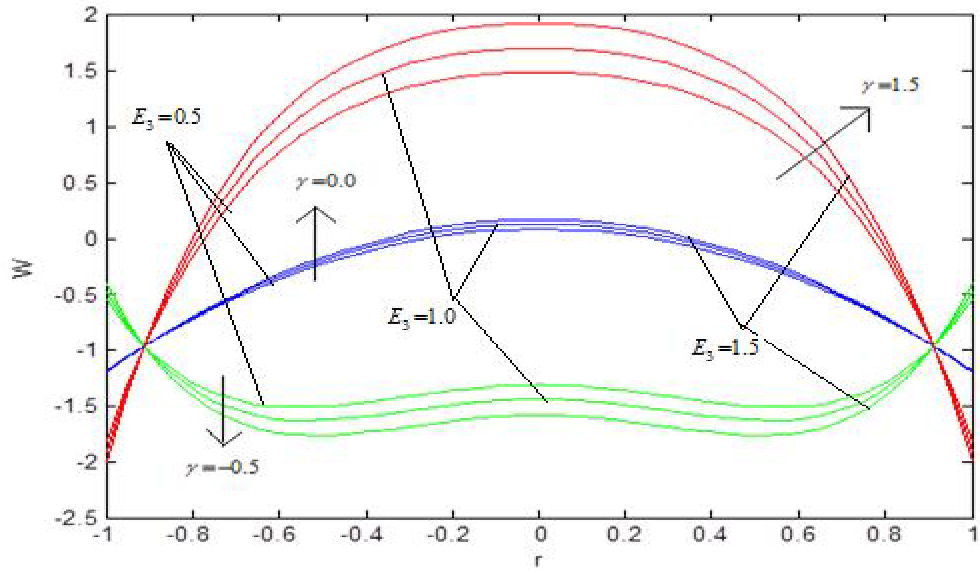

Figure 4. For fixed $E_2 = 1.5, E_3 = 0.5, \lambda = 0.02, z = 0.22, \varepsilon = 0.01, t = 0.25, l_2 = 0.34, k = 2.4$ varying $E_3 = 0.5, 1.0, 1.5,\ \gamma = -0.5, 0, 0.5$

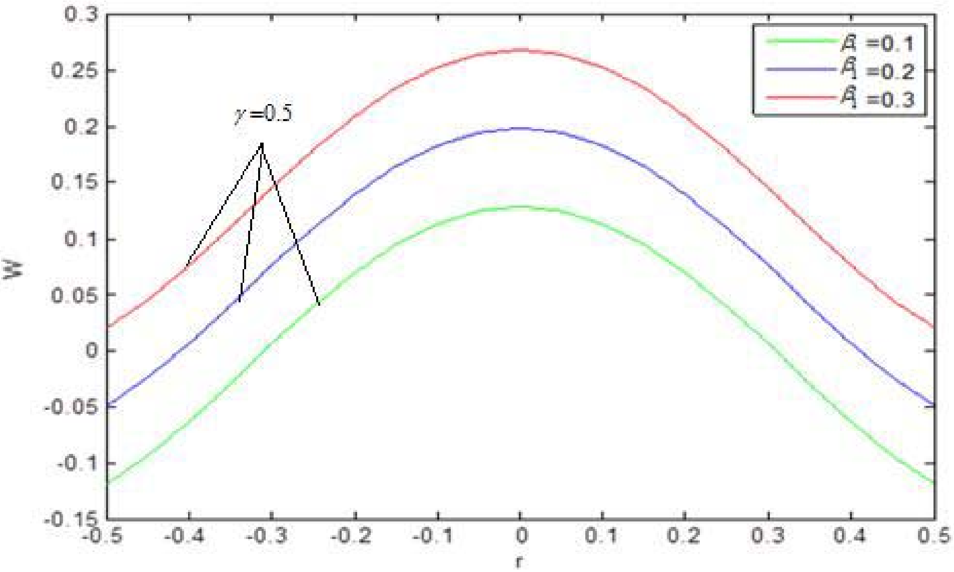

Figure 5. For fixed $E_1 = 0.5, E_2 = 1.0, E_3 = 1.5, \lambda = 0.02, z = 0.22, \varepsilon = 0.01, t = 0.25, l_2 = 0.34,$ $k = 2.4, \gamma = 0.5$ Varying $\beta_1 = 0.1, 0.2, 0.3$

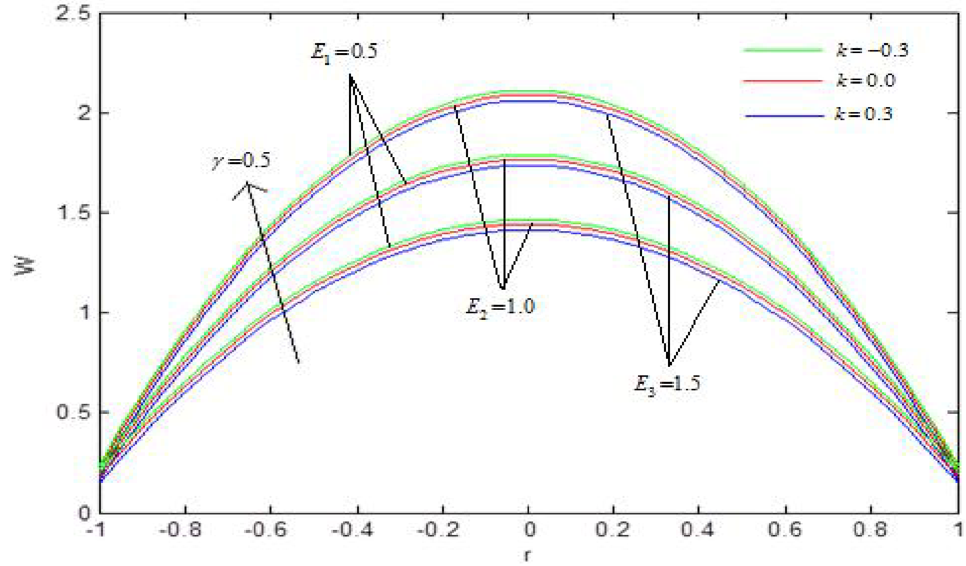

Figure 6. For fixed $E_1 = 0.5, E_2 = 1.0, E_3 = 1.5, \lambda = 0.02, z = 0.22, \varepsilon = 0.01, t = 0.25, l_2 = 0.34,$ $k = 2.4, \gamma = 0.5$ Varying $k = -0.3, 0.3, 0.3$

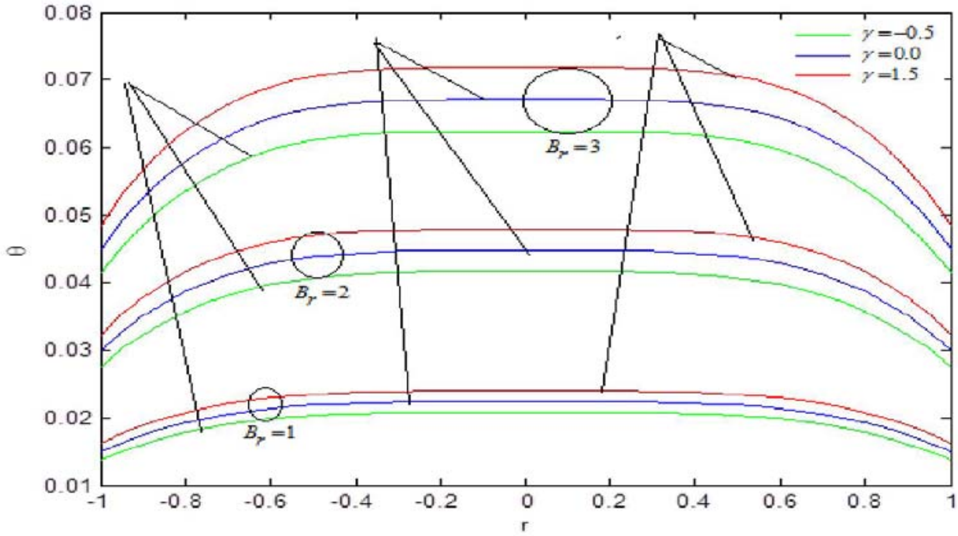

Figure 7. For fixed $E_1 = 1.0, E_2 = 1.5, E_3 = 0.5, \lambda = 0.07, z = 0.22, \varepsilon = 0.01, t = 0.25, l_2 = 0.24, k = 2$ Varying $\gamma = -0.5, \gamma = 0.0, \gamma = 1.5,$ $B_r = 1, 2, 3$

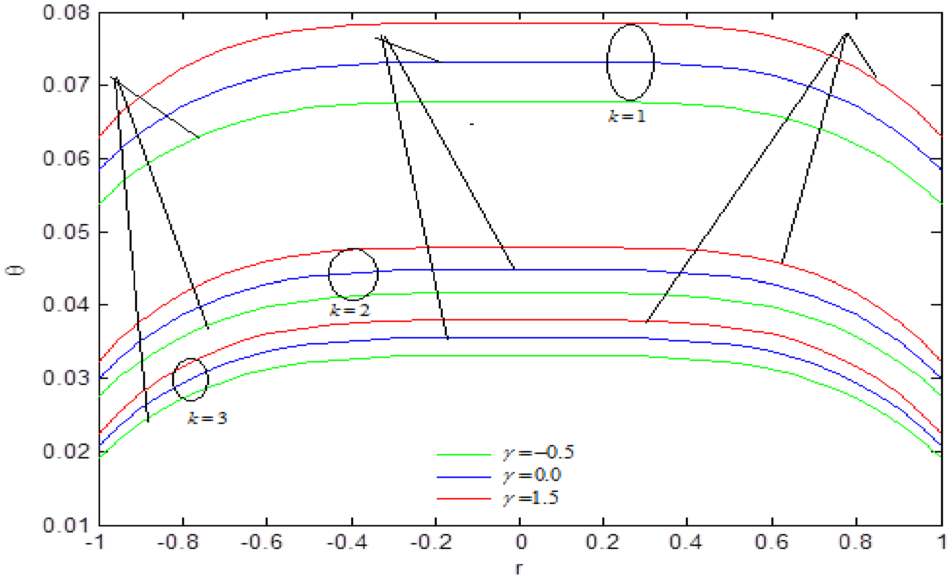

Figure 8. For fixed $E_1 = 1.0, E_2 = 1.5, E_3 = 0.5, \lambda = 0.07, z = 0.22, \varepsilon = 0.01, t = 0.25, l_2 = 0.24, B_r = 2$
Varying $\gamma = -0.5, \gamma = 0.0, \gamma = 1.5,\ k = 1, 2, 3$

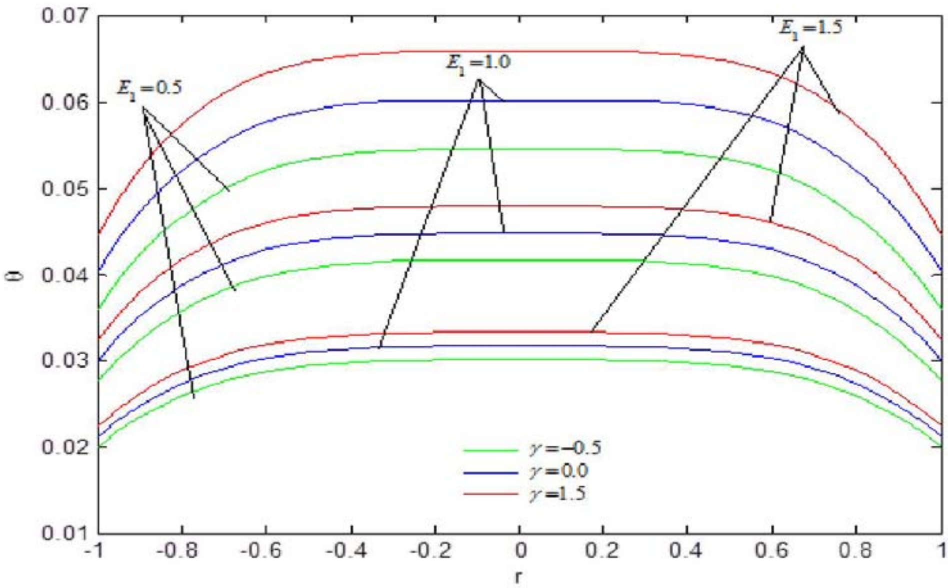

Figure 9. For fixed $E_2 = 1.5, E_3 = 0.5, \lambda = 0.07, z = 0.22, \varepsilon = 0.01, t = 0.25, l_2 = 0.24, B_r = 2, k = 2$
Varying $\gamma = -0.5, \gamma = 0.0, \gamma = 1.5,\ E_1 = 0.5, 1.0, 1.5$

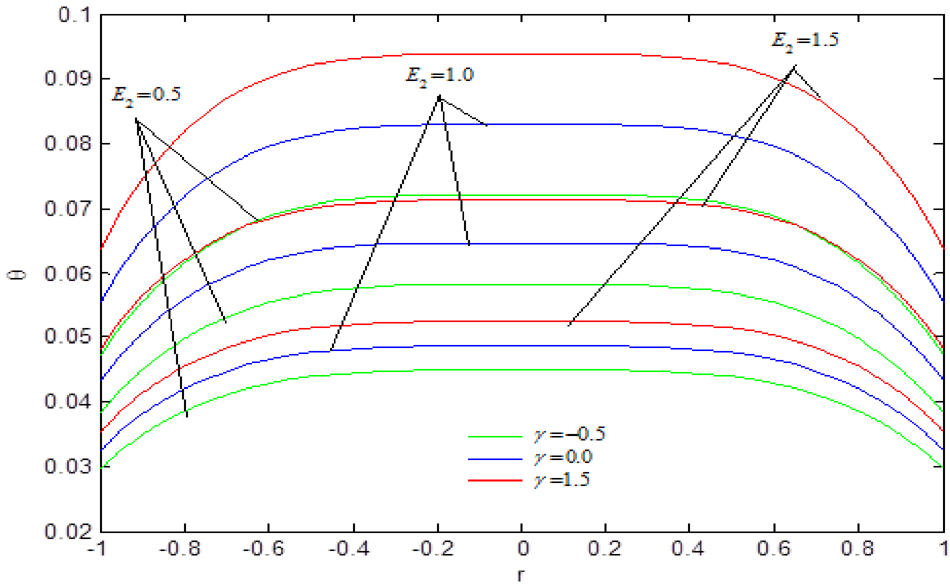

Figure 10. For fixed $E_1 = 1.5, E_3 = 1.0, \lambda = 0.07, z = 0.22, \varepsilon = 0.01, t = 0.25, l_2 = 0.24, B_r = 2, k = 2$ Varying $\gamma = -0.5, \gamma = 0.0, \gamma = 1.5,\ E_2 = 0.5, 1.0, 1.5$

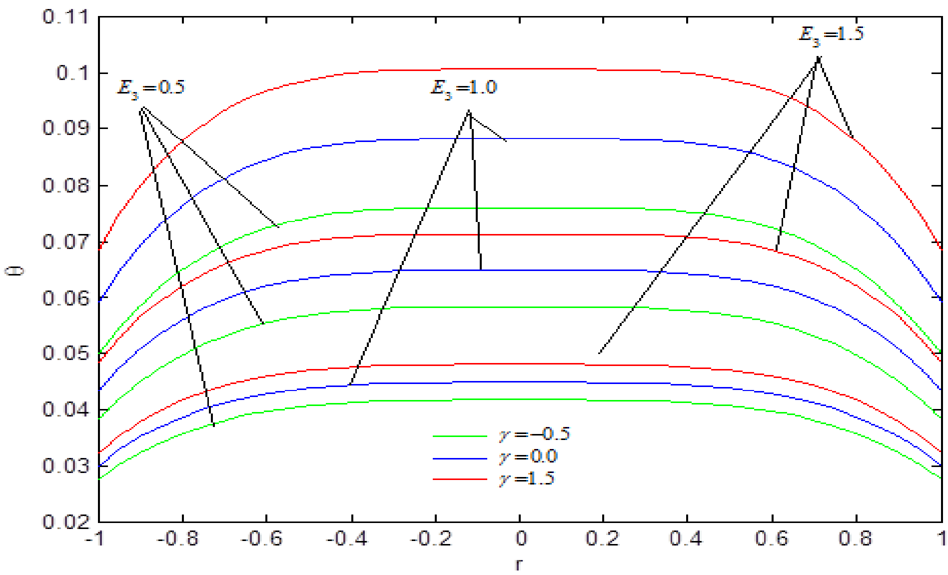

Figure 11. For fixed $E_1 = 1.5, E_2 = 1.0, \lambda = 0.07, z = 0.22, \varepsilon = 0.01, t = 0.25, l_2 = 0.24, B_r = 2, k = 2$ Varying $\gamma = -0.5, \gamma = 0.0, \gamma = 1.5,\ E_3 = 0.5, 1.0, 1.5$

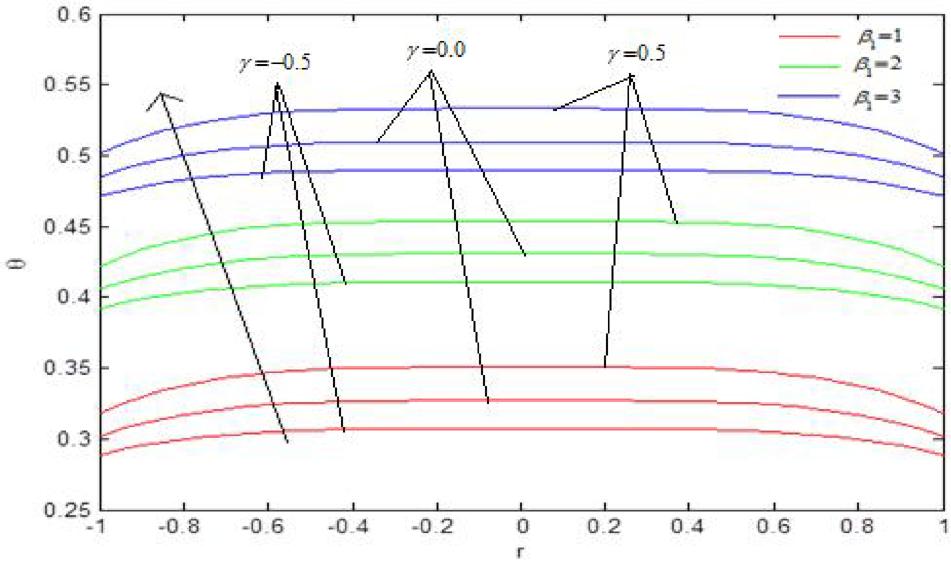

Figure 12. For fixed $E_1 = 1.5, E_2 = 1.0, E_3 = 0.5, \lambda = 0.07, z = 0.22, \varepsilon = 0.01, t = 0.25, l_2 = 0.24, B_r = 2$ $k = 0.2$ Varying $\gamma = -0.5, \gamma = 0.0, \gamma = 1.5,$ $\beta_1 = 1,2,3$

4. Conclusion

In the present study, we have discussed slip effects for peristaltic flow of Rabinowitsch fluid model in a non uniform tube. Exact solution is calculated for velocity and temperature profile.

1. The velocity profile increases for increasing values of rigidity parameter E_1 and stiffness parameter E_2, viscous damping force parameter E_3 for shear thinning and viscous cases, but, opposite behavior is depicted for shear thickening case because due to the elastic nature of the walls of the tube provides the less resistance to the fluid to flow.
2. The velocity profile increases for increasing of E_1, E_2 and E_3 with increasing of slip parameter β_1 and non uniform parameter k.
3. The temperature profile is increasing for increasing of Brickman number for shear thinning, shear thickening and viscous fluid. Physically larger values of B_r fluid temperature increases due to the stronger heat generation due to friction is used by shear in the flow which raises the fluid temperature.
4. For increasing the non-uniform parameter k decreases the thermal conductivity which contributes to the decrease in temperature profile.
5. The temperature profile is increasing with increasing of slip parameter β_1.

References

[1] Fung Y C and Yih C S 1968 *J. Fluid mech. Trans. ASME* **5** 669-675
[2] Shapiro A H, Jafferin M Y and Weinberg S L 1969 *J. Fluid Mech.* **37** 799-825
[3] Radhakrishnamacharya G 1982 Rheol. Acta **21** 30-35
[4] Misery A.M. EL.Shehawey E.F.EL. and Hakeem 1996 J.*Phys, Soc. Japan* **65(**11) 3524-3529
[5] Mishra M and Rao A R 2003 Z. *Ange math. Phy.* **54** 532-550

[6] Srinivasacharya D, Mishra M and Rao A R 2003 Acta Mech. **161** 165-178
[7] Hayat T, Wang Y, Hutter K , Asghar S, and Siddiqui A M 2004 *Math. Problems Eng* **4** 347-376
[8] Kothandapani M, Srinivas S, 2008 *Phs. Lett. A* **372** 4586-4591
[9] Sobh A M 2008 Turkish *J. Eng. Sci.* **32** 117-123
[10] Sinha A, Shit G C , Ranjit N K 2015 *Alexandria Eng. J.* **54** 691-704
[11] Kavitha A, Hemadri Reddy R 2012 *Int. J. Mech. Mate. Eng* **7(**2) 152-157
[12] Elda be N T , Elshaboury S M , Alfaisal A H . 2013 *Innovative Systems Design and Eng*. **3** 51-67
[13] Dheia G S , Ahmed M A 2014 Mathematical Theory and Modellng **4** 51-67
[14] Kavitha A , Hemadri reddy R 2015 *Ain Shams Eng. J*. **14**(2) 45-50
[15] Saravana R, Sreenadh S, Hemadri Reddy R *Int. J. Innov Tech. Creat. Eng.* 1 10-24
[16] Saravana R, Hemadri Reddy, Kavitha A Int. J.Appl. Math Mech. **9** 51- 86
[17] Saravana S, RH Reddy, Kavitha AMalaysian J. Mathematical Sciences 10 35-47
[18] Wada S, Hayashi H, 1971 *Bulletin of JSME* **69** 268-278
[19] Singh U P , Gupta R S and Kapur V K 2012 *Tribology in Industry* **34** 128-137
[20] Akbar N S and Nadeem S 2014 *Zeitschrift fir Naturforshung A,* **69** 473-480
[21] Bourgin P and Gay B 1984 *J. Tribology* **106** 285-290
[22] Hsu Y C, Saibel E 1965 *A S L E Transactions* **8** 191-194
[23] Maraj E N and Nadeem S 2015 *Zeitschrift fir Naturosroschun g A*, **70** 513-520
[24] Singh B K and Singh U P 2014 *Int. J. Fluids Eng.* **6**(1) 1-8
[25] Noreen Akbar, Adil Wahid Butt, Heat *transfer analysis Rabinowitsch fluid due to metachronal wave of cilia*, 2211-3797-2015, Published by Elsevier B.V. under CC BY-NC-ND.
[26] Sinha A, Shit G C, Ranjit N K 2015 *Alexandria Eng. J.* **54** 691-704
[27] Eldabe N T, Elshaboury S M, Alfaisal A H 2012 *Innovative Systems Design and Engineering,***3** 51-67